Journal of Electron Spectroscopy and Related Phenomena, 68 (1994) 347–355
0368-2048/94/$07.00

Electronic and Geometric Structure of Adsorbates on Oxide Surfaces

D. Cappus, M. Menges, C. Xu, D. Ehrlich, B. Dillmann, C.A. Ventrice Jr., J. Libuda, M. Bäumer, S. Wohlrab, F. Winkelmann, H. Kuhlenbeck, H.-J. Freund

Lehrstuhl für Physikalische Chemie I, Ruhr-Universität Bochum
Universitätsstr. 150, 44780 Bochum, Germany

We have investigated the electronic and geometric structure of surfaces of transition metal oxides and simple metal oxides applying electron spectroscopic methods. In order to avoid charging problems, we have resorted to the preparation of thin (5 - 50 Å) metal oxide films grown on metallic substrates via several oxidation techniques. We have studied NiO, CoO, Cr_2O_3, and Al_2O_3. The thin films have the advantage that they may be easily cooled to liquid nitrogen and liquid helium temperatures. Another interesting feature of the thin films is the possibility to prepare thermodynamically unstable surfaces, such as (111) surfaces of ionic rock salt structures, and study the adsorption and reaction at such surfaces. Adsorption and reaction of molecules has not only been investigated on the clean oxide substrates but also on the surfaces modified through deposited ultrathin metal films. Such systems may be considered as models for heterogeneous catalysts.

1. Introduction

Heterogenous catalysts often are based on transition metal oxides as the active components or on simple metal oxides which are used as supports for deposited ultrathin transition metal films. For a long period of time surface science has tried to develop model systems to understand the mechanisms of the reactions on a microscopic level. The most spectacular successes in this field have been achieved by choosing single crystal metal surfaces, as the appropriate substrates applying electron spectroscopic methods [1,2]. One example is the Haber-Bosch-reaction for the synthesis of ammonia from elemental nitrogen and hydrogen [3]. Also, the influence of additives such as alkali metals, sulphur and halogens on this reaction have been investigated [4]. Less often oxide surfaces have been used as model systems [5,6]. On such surfaces transition metals have been deposited and adsorption of molecules on the composite system has been studied [7,8].

Surface science investigations of adsorption on insulating oxide surfaces have only been moderately successful partly probably due to the charging and cooling problems occuring for these systems, especially when bulk oxide materials, whether single crystals or powders are used.

It has therefore been one of our goals to prepare thin, well ordered oxide films on metal substrates which do not charge upon electron impact or electron emission, and which can easily be cooled to liquid nitrogen or even liquid helium temperatures. Transition metal oxides with different surface structures, i.e. rock salt (100) and (111) surfaces [9,14] as well as corundum (111) planes [15-20] have been prepared. The clean surfaces are characterized by highly localized surface states probed by electron energy loss spectroscopy [13,15]. These states strongly react towards the presence of atomic and molecular adsorbates. We show that different adsorbed molecules, for example OH and NO, preferentially interact with different parts of the surface of the films. This allows us to differentiate between terrace and defect sites [12].

Ultrathin metal films deposited on the thin oxide films exhibit different behaviour with respect to surface wetting. While an Al_2O_3 surface is not wetted by Ag [7], Pt deposits exhibit strong interaction at room temperature leading to surface wetting [21]. It is shown that Pt diffuses into the Al_2O_3 film [22]. Consequences for the adsorption of

SSDI 0368-2048(94)02133-K

molecules due to the strong Al_2O_3-Pt interaction are discussed.

2. Experimental

For this study three different UHV systems have been used. Two systems contain hemispherical electron energy analysers rotable in two orthogonal planes for angle resolved electron detection or fixed analysers for X-ray Photoelectron Spectroscopy (XPS). One of these systems is additionally equipped with a hemispherical electron monochromator for angle resolved EELS (Electron Energy Loss Spectroscopy). The third system contains an EELS setup consisting of a double pass cylindrical electron analyser and monochromator. Additionally, all systems are equipped with LEED (Low Energy Electron Diffraction) systems, quadrupole mass spectrometers for residual gas analysis and TDS, and ion guns for sample preparation.

The metallic samples which were used for the preparation of the thin film oxides were spot welded to two tungsten rods which were connected to a liquid nitrogen reservoir. With this arrangement temperatures below T = 100 K could be reached. A tungsten filament was mounted behind the samples which could be used for sample heating by electron impact or radiative heating. The samples were cleaned by repeated cycles of etching with Ne ions and annealing.

Studies on the oxidation of Ni have been performed rather early by Conrad et al. [23]. The NiO(100) and NiO(111) films have been prepared by oxidation of Ni(100) and Ni(111) single crystal surfaces in an oxygen atmosphere. NiO(100) was grown by cycles of oxidation with 1000 L (1 L = 10^{-6} torr sec) of O_2 at elevated temperature (T = 570 K) followed by annealing at T = 650 K. These cycles were repeated until the LEED pattern indicated the formation of an ordered oxide film. The NiO(111) layers were prepared in a similar way. Both types of oxide films exhibit an appreciable amount of defects as indicated by the rather high background intensity and by the large half widths of the spots in the LEED patterns.

Immediately after preparation the NiO(100) and NiO(111) films were found to be covered with OH groups, compatible with the H_2O and H_2 background pressure. These could be removed by annealing at T = 600 K. After cooling down, the formation of OH species could be observed again, indicating that the hydroxyl species were formed by a reaction of the oxide surfaces with the residual gas atmosphere. For the isotope exchange experiments the hydroxylated oxide films were briefly flashed to T = 600 K in an atmosphere of 10^{-6} mbar of D_2O.

Some experiments have also been performed with a NiO(100) single crystal surface. The single crystal rod was cleaved in vacuo. This procedure resulted in a well ordered (100) surface with a very small concentration of defects which gave rise to a sharp (1x1) LEED pattern with low background intensity. On the cleaved surface no OH formation in detectable amounts was observed. Since the thermal contact of the single crystal rod to the sample holder was not as good as for the spot welded metal samples we used a helium cryostate for cooling purposes.

The Cr_2O_3(111) films were prepared by oxidation of a Cr(110) single crystal surface. For this purpose the Cr(110) sample was annealed at T = 500 K in an atmosphere of 10^{-6} mbar of O_2 for 3 minutes. After this treatment the sample was annealed at T = 1000 K in order to remove excess oxygen from the surface. The LEED pattern of the oxide film exhibits a hexagonal symmetry as expected for Cr_2O_3(111).

The aluminum oxide samples were prepared in the following way: after cleaning the NiAl(110) sample using sputtering and annealing cycles, the oxide film was prepared by admitting 1200 L of oxygen at T = 550 K into the chamber, and subsequent annealing to 1200 K as described in more detail elsewhere [19]. The quality of the resulting oxide film was documented by a set of sharp LEED spots with low background intensity.

Metal has been deposited from a Knudsen cell in the case of Ag and from a metal filament in the case of Pt. The coverage was controlled via a quartz balance and checked with XPS.

3. Results and Discussion

A (100) surface of nickel oxide with rock salt structure is schematically shown in Fig. 1. Each

metal ion in the surface, for example, is surrounded by five nearest neighbours, while in the bulk it has six nearest neighbours in octahedral symmetry. Globally speaking, this leads to a reduction of the ligand field strength in the surface as compared with the bulk and hence to a smaller splitting in the 3d-levels. Consequently, d-d excitations of surface Ni atoms are expected to have lower energies with respect to Ni atoms in the bulk. It should, therefore, be possible to differentiate between surface and bulk transitions. Figure 2 shows a set of EEL spectra. The lowest spectrum has been taken on an in vacuo cleaved NiO(100) surface. The hatched bands are due to excitations localized in the surface, the other bands are caused by bulk transitions. A very similar situation is encountered in the case of thin NiO(100) films grown on a Ni(100) single crystal substrate (2nd spectrum from bottom). However, in contrast to the in situ cleaved single crystal, the film is susceptable to adsorption of H_2O from the residual gas, as indicated in Fig. 2 by the pronounced vibrational OH losses overlapping the surface excitations at 0.6 eV. We identify through isotope exchange experiments the nature of these losses as shown in the spectrum by the attenuation of the OH loss and appearance of an OD loss. We had concluded before that this is an indication of OH adsorption on defects present on the film [12]. We know from LEED and STM investigations that about 25% of the film surface is covered by defects [10,11] on which it is obviously possible to dissociate H_2O. The terrace sites on the perfect crystals on the other hand do not induce H_2O dissociation [24]. If we expose, however, an OH saturated film to NO, this molecule shifts the surface excited state (top spectrum) [13]. Since the surface excitations are characteristic for the ideal Ni sites on the terraces, this observation is conclusive evidence that the NO molecules adsorb onto these Ni sites, completing the coordination sphere and shifting the surface excitations to higher energies close to the bulk values (see Fig. 1). Lines are included in Fig. 2 to guide the eye.

The existence of OH and NO on the surface is also documented by XPS. XP spectra in the O1s and N1s range [9-12,14] are shown in Fig. 3. The O1s spectrum of the cleaved NiO single crystal shows a symmetric single O1s line [14]. An OH-saturated NiO(100) surface exhibits a small shoulder at 2 eV higher binding energies [12]. The intensity ratios between OH induced line and main O1s line are compatible with the coverage of 25 - 30% of the surface as deduced from LEED and STM for the percentage of the defect covered surface [9,11].

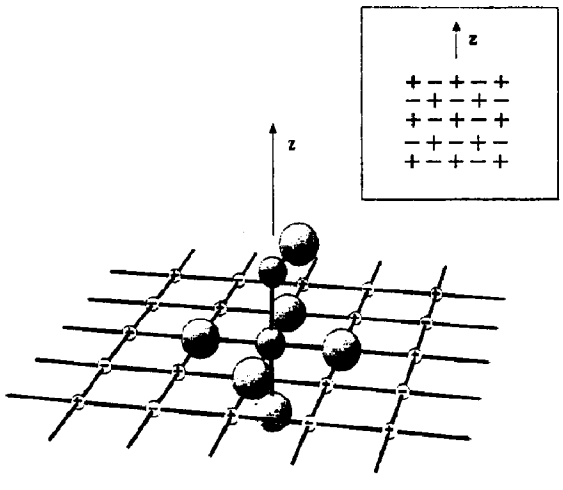

Fig. 1. Schematic drawing of a NiO_5 cluster in the surface of an ionic NiO bulk crystal. A NO molecule has been coordinated to the Ni atom in the culster. The geometry of the Ni-NO bond has been taken from NEXAFS data [9].

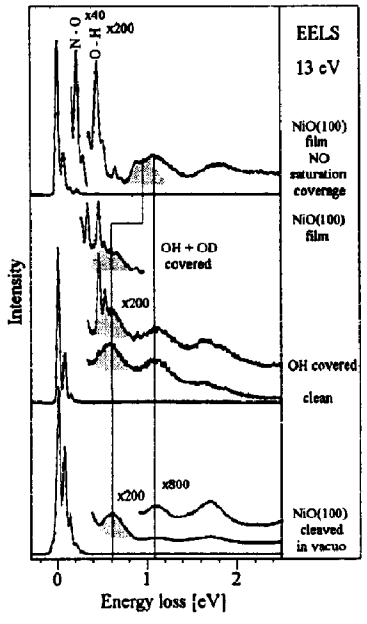

Fig. 2. Electron energy loss spectra of various NiO samples without and with adsorbates.

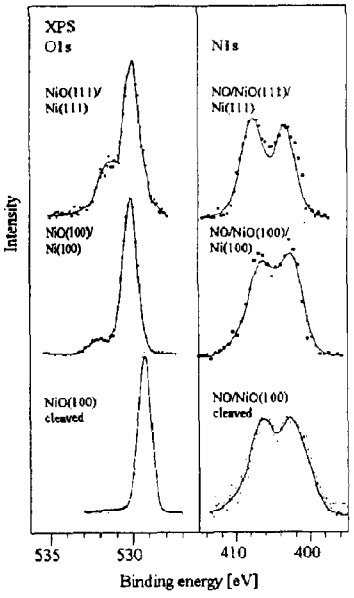

Fig. 3. X-ray Photoelectron Spectra of clean (left) NO covered (right) NiO samples in the ranges of the O1s ionization ("clean" samples) and the N1s ionization (NO covered samples). O1s spectra have been taken at grazing excidence.

What is the nature of the defects that are associated with the dissociation of H_2O? Figure 4 schematically shows a possibility : The (100) film (Fig. 4a) consists of larger (100) terraces which are separated by smaller regions of (111) and (100) orientation. In the case of the (111) oriented faces the areas may be either Ni or O terminated. Is it possible that these (111) patches are responsible for the reactivity towards H_2O? One way to test this is to prepare NiO surfaces with predominant (111) orientation as schematically shown in Fig. 4b. Figure 3 shows the O1s spectrum of such a surface and it is obvious that the relative intensity of the high binding energy feature has considerably increased indicating an OH coverage on the (111) surface of about a factor of 2 larger. The structural quality of the NiO(111) films is rather better than worse if compared to the NiO(100) films. Therefore, the observed reactivity is due to the (111) patches and thus we may conclude that the (111) patches are possible candidates to explain the observed defect induced H_2O dissociation on NiO(100).

The NO N1s spectra exhibit two bands separated by 5 eV as shown in Fig. 3. Since TDS [9-12] proves the presence of a single majority species it is very likely that this splitting is due to giant shake up, so far only observed for molecules weakly adsorbed on metal surfaces [25-28]. Briefly, the core hole created may be either unscreened, i.e. the hole resides on the NO molecules, or screened where a hole resides on the NiO substrate. In other words, in the ionisation process an electron has been transferred from the substrate to the NO molecule, which leads to a hole state more stable than the unscreened state, consequently appearing at lower binding energy [9]. This qualitative interpretation has recently been reinforced via *ab-initio* calculations by Petterson [29].

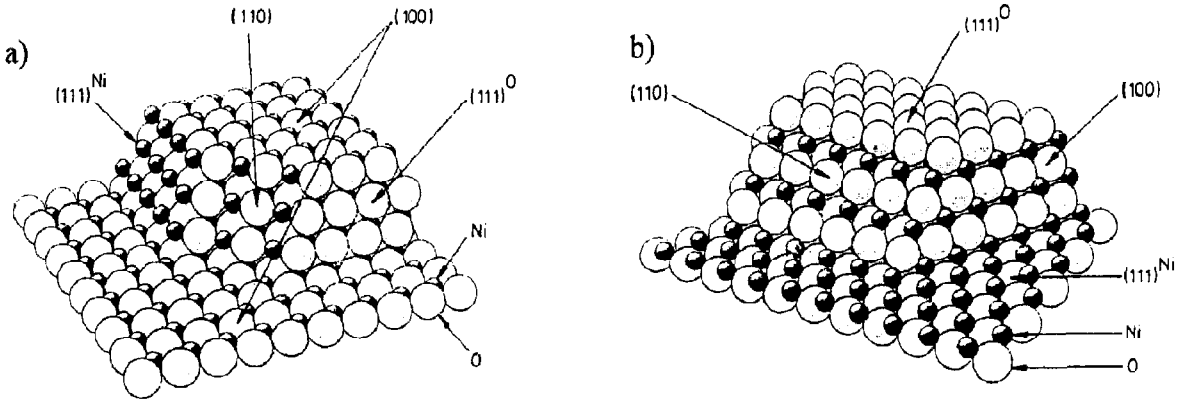

Fig. 4. a) Schematic drawing of a facetted NiO(100) surface. The facets expose Ni terminated, O terminated (111) planes and (110) planes.
b) Schematic drawing of a facetted NiO(111) surface. The facet expose (100) and (110) planes. The lower and the upper (111) terrace are Ni and O terminated, respectively.

Thermal desorption investigations of NO adsorption and desorption on NiO (100) in comparison with NiO(111) have been presented and discussed recently [12]. These studies indicate that, when the (111) films are dehydroxylated, they also exhibit a stronger reactivity towards NO. In contrast to NiO(100) where we observe only a single molecular species desorbing from the terraces around 220 K, and a minority species possibly connected with residual defect adsorption, we find several desorbing NO species on the dehydroxylated NiO(111) surface including one which possibly desorbs out of adsorbed NO_2 molecules above 400 K [12].

Another interesting, but rather different case of a transition metal oxide surface is represented by the Cr_2O_3(111) surface [15-17]. We have previously looked at adsorption on this surface and know that this system is characterized by an electronic excited surface state. Upon interaction with various molecules from the gas phase, this state was considerably influenced in its intensity. We have studied the corresponding energy range again in more detail. Figure 5 shows the electron energy loss spectra up to about 2.5 eV loss energy. Three features are found at 1.2 eV, 1.4 eV, and 1.75 eV.

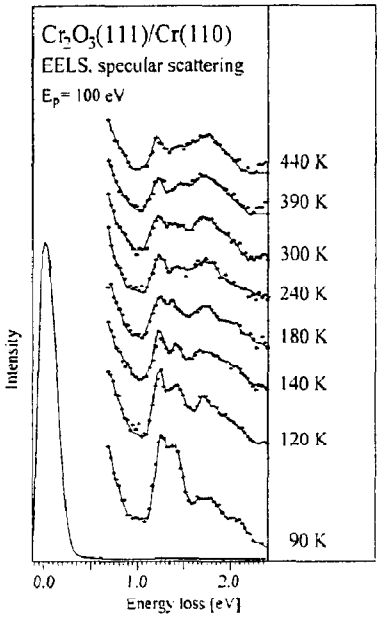

Fig. 5. Electron energy loss spectra of the clean Cr_2O_3(111)/Cr(110) surface at various temperatures and a primary electron energy of 100 eV.

We have argued before [15-16] that the losses above 1.5 eV are due to excitation of the Cr^{3+} ions in Cr_2O_3. In fact, the loss at 1.75 eV is due to the excitation from the $^4A_{2g}$ ground state of Cr^{3+} to the ^2E_g and $^2T_{1g}$ states, i.e. the famous ruby line. The losses at lower energies cannot be due to transitions on Cr^{3+} ions in a regular bulk Cr_2O_3 ligand field. One possibility would be the assignment of the band to the excitation of Cr^{3+} ions in a reduced ligand field, a situation encountered at the surface of Cr_2O_3 similar to the discussion for NiO given above. Another possibility is that the transitions occur on Cr^{2+} ions present in the surface as discussed earlier [15-16]. An argument in favour of a charge reduced state is the electrostatic stabilization the polar Cr_2O_3(111) surface experiences in this case [15-16]. A definite assignment is not straightforward and it is even more involved if we realize that the relative intensities of the 1.2 eV/1.4 eV losses with respect to the 1.75 eV loss change with surface temperature as shown in Fig. 5. This latter effect may have several reasons, including magnetic as well as dynamic effects, i.e. atomic motion in the surface. It is clear, however, that the low energy losses are

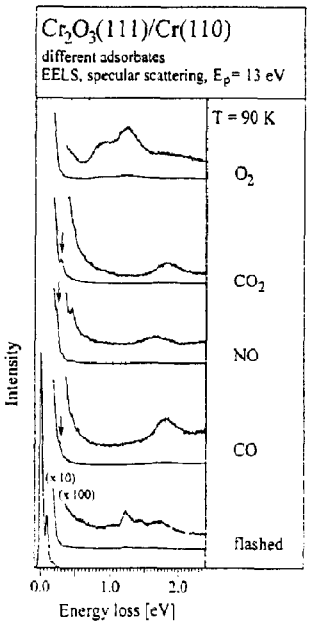

Fig. 6. Electron energy loss spectra of the clean and adsorbate covered (flashed) Cr_2O_3(111)/Cr(110) surface at a primary electron energy of 13 eV and a surface temperature of 90 K. Saturation coverage was achieved.

localized in the surface region because they are very sensitive towards the presence of adsorbates. Figure 6 shows the loss region for several adsorbates on Cr_2O_3. In some cases the vibrational losses of the adsorbates are observed (arrows). The 1.2 eV/1.4 eV loss is quenched in all cases. In the case of the O_2 adsorbate the situation is more complicated. The extra features are connected with molecular oxygen on the surface. However, the definitive assignment is not straigthforward. O_2 desorbs from the surface between 180 K and 210 K with two maxima in the TD spectra [16]. After the desorption has taken place the two extra features are gone but the 1.2 eV and 1.4 eV losses are still quenched [30]. The vibrational loss spectrum indicates the presence of a species with vibrational frequency around 1000 cm^{-1} which we have assigned before [16] to the formation of a chromyl species. After flashing the surface the 1.2 eV and 1.4 eV losses reappear. Obviously, the Cr_2O_3 has a rich surface chemistry which may be interesting to study in more detail in the future.

So far we have only discussed the interaction between gases and pure oxide surfaces. In the next example we consider Al_2O_3, which in its pure form only very weakly interacts with the gas phase. However, Al_2O_3 is often used as a support material onto which transition metals are deposited, sometimes with a well defined metal dispersion [8]. Such systems can be highly active as heterogenous catalysts [8]. We have tried to model the step of metal deposition by choosing Pt as the deposit. We have deposited Pt in submonolayer and higher coverages onto an Al_2O_3 thin film surface grown on a NiAl(110) substrate [18-20]. We know from Auger [31], XPS [32] and LEED [21] that this film is not thicker than 5 Å and covers the NiAl(110) surface completely as revealed by CO titration experiments (see below) [22]. The LEED pattern of such a film is very sharp as shown in Fig. 7. Its analysis reveals that the structure grows in two domains and the terrace width is of the order of 200 Å [19,20]. A more detailed account of the LEED analysis will be given elsewhere [21]. The topmost oxygen layer has most probably quasi hexagonal symmetry and contains very little if any OH [7,18-20]. Figure 8 shows a set of EEL spectra in the range of surface phonons, so called Fuchs-Kliewer-phonons, of the Al_2O_3 substrate. The trace of the

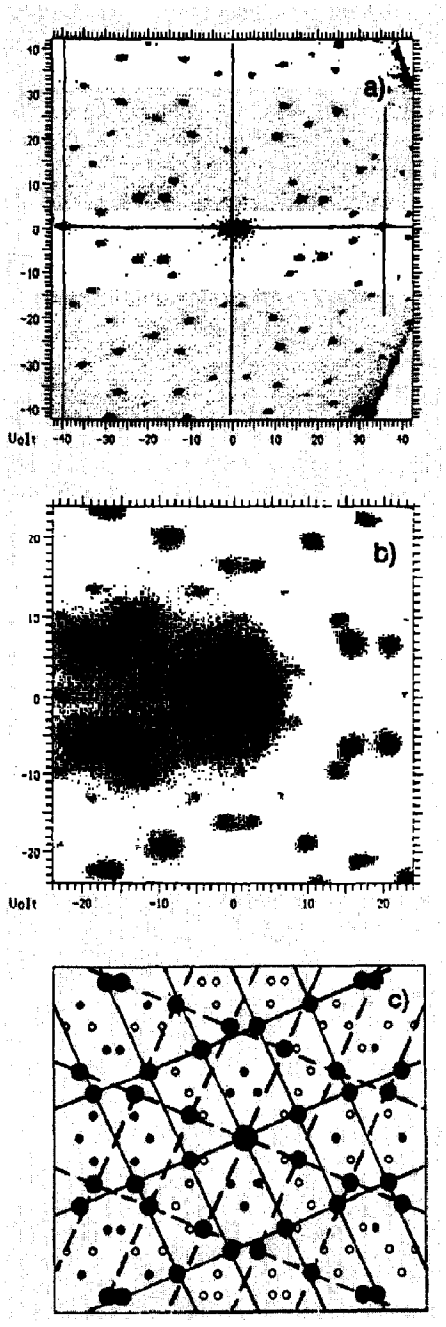

Fig. 7. SPA-LEED pattern of Al_2O_3(111)/ NiAl(110)
a) overview.
b) enlarged view with Al_2O_3 unit cell.
c) schematic representation indicating the two domains.

clean substrate exhibits three phonons which have been discussed earlier [18] and which indicate that the substrafe is not of α-Al_2O_3 type but rather of γ-Al_2O_3 type. In α-Al_2O_3 the Al ions exclusively occupy octahedral sites within the hexagonal oxygen sublattice while in γ-Al_2O_3 also tetrahedral sites in a cubic oxygen lattice are occupied. However, not all sites are populated but their occupancy is at random. The Al_2O_3 film adsorbs CO below 70 K and mono- as well as multilayer growth including different adsorbate states may be differentiated [19,20]. In EELS the electronically excited states of the adsorbed molecules may be observed even in the monolayer regime [19,20]. The excitation energies and the vibrational structure observed are indicative of a physisorbed molecule with very limited distortion of its electronic and geometric structure from the gas phase [19,20].

If we deposit a transition metal, as for example Pt, at room temperature on the surface the properties of the system change considerably. The

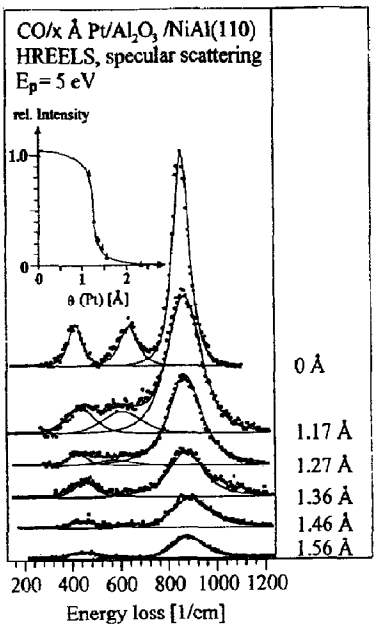

Fig. 8. Electron energy loss spectra of the phonon range of Al_2O_3(111)/NiAl(110). The spectrum of the clean system is compared with the spectra of the system on which various amounts of Pt have been deposited. .The inset shows the intensity of the leading Al_2O_3 phonon as the function of metal layer thickness.

phonons of the system as shown in Fig. 8 broaden and are strongly attenuated. At the same time the LEED pattern becomes more and more diffuse [21], and at about $\Theta_{Pt} = 0.2$ has completely vanished. A spot profile analysis of the (0,0)-reflex, recently carried out in our laboratory [21], has revealed that Pt wets the Al_2O_3 surface at this temperature and each Pt atom structurally influences a range of about 12 Å in diameter of the Al_2O_3 surface being equivalent to seven oxygen species in the quasihexagonal surface. Upon heat treatment the Pt migrates through the Al_2O_3 film and eventually the structure of the oxide is reestablished.

The broadening and attenuation of the phonons (Fig. 8) is connected with the formation of a metallic Pt film on the dielectric substrate. Such a behaviour has also been observed before for other systems. As may be deduced from the degree of attenuation of the Al_2O_3 phonons as shown in the inset in Fig. 8, a single monolayer of Pt leads to an almost complete quenching of the phonon losses indicating the formation of a 2 Å film with the response of a metal.

The adsorption properties of the thin Pt film are in certain aspects very similar to a Pt(111) surface as is revealed via EELS and TPD. Figure 9 shows the range of the CO stretching frequencies of the Pt/Al_2O_3 system dosed to saturation with CO. The observed frequency indicates CO molecules bound on-top on the surface [33]. At higher Pt coverages the band shifts and a second feature appears in the range of bridging CO sites [33]. Due to the relatively low resolution we cannot decide at present how many different chemical species contribute to the broad feature present at the lowest Pt coverage. The existence of several species is very likely and also revealed through TDS measurements. A series is shown in Fig. 10. There is a broad structure between 350 K and 550 K which shifts its maximum towards 450 K as the Pt coverage increases, and at high Pt coverage we find features known from TDS spectra taken on Pt(111) [34] and stepped Pt(335) [35] surfaces shown for comparison. However, there is a pronounced TDS feature slightly above a desorption temperature of 150 K which is not compatible with CO desorbing from metallic Pt. On the other hand we have found for CO desorbing from transition metal oxide surfaces maximum desorption temperatures between

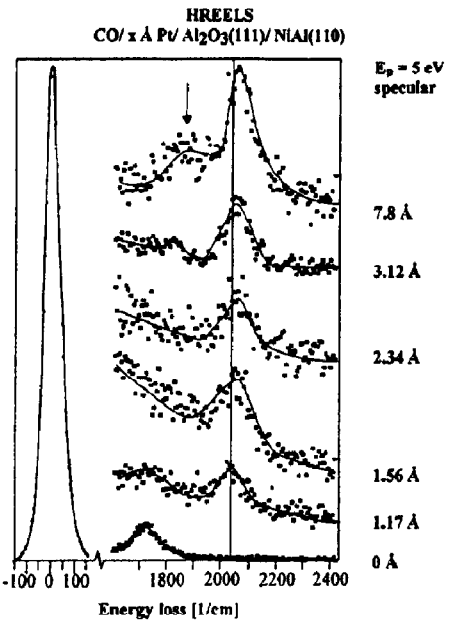

Fig. 9. Electron energy loss spectra in the range of the CO stretching frequency for various Pt coverages and CO saturation coverage Ep = 5 eV of the system Al_2O_3(111)/NiAl(110)

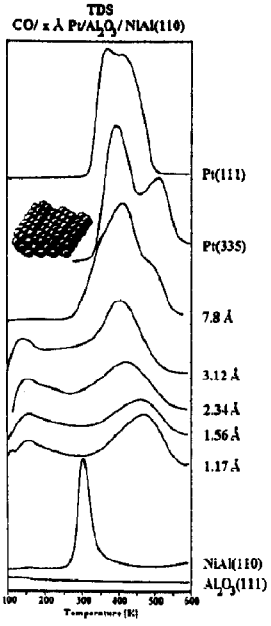

Fig. 10. Thermal desorption spectra of CO desorbing from $Pt/Al_2O_3(111)/NiAl(110)$. For comparison the TD-spectra of a stepped Pt(335) surface [35] and the smooth Pt(111) [34] surface are included. The two spectra at the bottom refer to the clean NiAl(110) substrate and the clean $Al_2O_3(111)/NiAl(110)$ substrate. The latter does not adsorb CO above 100 K.

100 K and 200 K [9,12,16]. It is therefore not unlikely that these CO species desorb from sites where a Pt atom has been incorporated into the first layer of the Al_2O_3. By comparison with the clean NiAl(110) substrate and the completely Al_2O_3 covered NiAl(110) which are included in Fig. 10 it is clear that the desorption maximum around 140 K cannot be connected with the metallic NiAl(110) substrate. An investigation of the chemical shift of the Pt/Al_2O_3 system measured via XPS reveals that the Pt is oxidized when it diffuses into the substrate [22]. One may speculate that the defect structure of the γ-Al_2O_3 substrate helps to facilitate the diffusion of the relatively smaller Pt ions into the quasihexagonal top oxygen layer of the Al_2O_3.

We have just begun to study reactions with this Pt/Al_2O_3/NiAl system. We have observed dissociation of CO at room temperature on these systems. This is in contrast to the clean Pt surfaces where at room temperature dissociation has not been observed. Where and how mechanistically this reaction occurs is not clear at present but our future research will be directed towards the study of reactions.

Acknowledgements

Our research has been supported by various agencies which are gratefully acknowledged: Deutsche Forschungsgemeinschaft, Ministerium für Wissenschaft und Forschung des Landes Nordrhein-Westfalen, Bundesministerium für Forschung und Technologie, European Communities and Fonds der Chemischen Industrie.

References

1. G. Ertl, J. Küppers "Low Energy Electrons and Surface Chemistry" Verlag Chemie, Weinheim 1988
2. D.A. King, D.P. Woodruff (Eds.) "The Chemical Physics of Solid Surfaces and Heterogeneous Catalysis" Vol. 1 - Vol. 4, Elsevier 1990

3. G. Ertl, Angew. Chem. 102, 1258 (1990)
4. M.P. Kiskinova "Poisoning and Promotion in Catalysis Based on Surface Science Concepts and Experiments", "Studies in Surface Science and Catalysis" Vol. 45, Elsevier 1989
5. H.H. Kung, "Transition Metal Oxides: Surface chemistry and catalysis", "Studies in Surface Science and Catalysis" Vol. 45, Elsevier 1989
6. H.-J. Freund, E. Umbach (Eds.) "Adsorption on ordered surfaces of ionic solids and thin films" Springer Series in Surface Science, in press
7. H.-J. Freund, B. Dillmann, D. Ehrlich, M. Haßel, R.M. Jaeger, H. Kuhlenbeck, C.A. Ventrice, F. Winkelmann, S. Wohlrab, C. Xu, Th. Bertram, A. Brodde, H. Neddermeyer, J. Mol. Catal. 82, 143 (1993)
8. R. Burch, Catalysis 7, 143 (1985)
9. H. Kuhlenbeck, G. Odörfer, R.M. Jaeger, G. Illing, M. Menges, Th. Mull, H.-J. Freund, M. Pöhlchen, V. Staemmler, S. Witzel, C. Scharfschwerdt, K. Wennemann, T. Liedtke, and M. Neumann, Phys. Rev. B43, 1969 (1991)
10. M. Bäumer, D. Cappus, G. Illing, H. Kuhlenbeck, H.-J. Freund, J. Vac. Sci. Technol. A10, 2407 (1992)
11. M. Bäumer, D. Cappus, H. Kuhlenbeck, and H.-J. Freund, G. Wilhelmi, A. Brodde, H. Neddermeyer, Surf. Sci. 253, 116 (1991)
12. D. Cappus, C. Xu, D. Ehrlich, B. Dillmann, C.A. Ventrice Jr., K. Al-Shamery, H. Kuhlenbeck, H.-J. Freund, Chem. Phys., in press
13. A. Freitag, V. Staemmler, D. Cappus, C.A. Ventrice Jr., K. Al-Shamery, H. Kuhlenbeck, H.-J. Freund, Chem. Phys. Lett., in press
14. S. Uhlenbrock, C. Schwarfschwerdt, M. Neumann, G. Illing, H.-J. Freund, J. Phys.: Condens. Matter 4, 7973 (1992)
15. C. Xu, B. Dillmann, H. Kuhlenbeck, H.-J. Freund, Phys. Rev. Lett. 67, 3551 (1991)
16. H. Kuhlenbeck, C. Xu, B. Dillmann, M. Haßel, B. Adam, D. Ehrlich, S. Wohlrab, H.-J. Freund, U.A. Ditzinger, H. Neddermeyer, M. Neuber, M. Neumann, Ber. Bunsenges. Phys. Chem. 96, 15 (1992)
17. C. Xu, M. Haßel, H.Kuhlenbeck, H.-J. Freund, Surf. Sci. 258, 23 (1991)
18. R.M. Jaeger, H. Kuhlenbeck, H.-J. Freund, M. Wuttig, W. Hoffmann, R. Franchy, H. Ibach, Surf. Sci. 259, 235 (1991)
19. R.M. Jaeger, H. Kuhlenbeck, H.-J. Freund, Chem. Phys. Lett. 203, 41 (1993)
20. R.M. Jaeger, J. Libuda, M. Bäumer, K. Homann, H. Kuhlenbeck, H.-J. Freund, J. Electr. Spectr. Rel. Phen., in press
21. J. Libuda, M. Bäumer, H.-J. Freund, unpublished
22. F. Winkelmann, S. Wohlrab, H.-J. Freund, unpublished
23. H. Conrad, G. Ertl, J. Küppers, E.E. Latta, Solid State Commun. 17, 497 (1975)
24. H.-J. Freund, H. Kuhlenbeck, M. Neumann, in "Adsorption on ordered surfaces of ionic solids and thin films" (H.-J. Freund, E. Umbach, Eds.) Springer Series in Surface Science, in press
25. H.-J. Freund, E.W. Plummer, Phys. Rev. B23, 4851 (1981)
26. R.P. Messmer, S.H. Lamson, Chem. Phys. Lett. 65, 465 (1979)
27. E. Umbach, Surf. Sci. 117, 482 (1982); Solid State Commun. 51, 365 (1984)
28. J.C. Fuggle, E. Umbach, D. Menzel, K. Wandelt, C.R. Brundle, Solid. State Commun. 27, 65 (1978)
29. L.G.M. Petterson, Theor. Chem. Acta, in press
30. D. Ehrlich, H. Kuhlenbeck, H.-J. Freund, unpublished
31. H. Isern, G.R. Castro, Surf. Sci. 211/212, 865 (1989)
32. B. Adam, H.-J. Freund, unpublished
33. H. Ibach, D.L. Mils, Electron Energy Loss Spectroscopy and Surface Vibrations, Academic Press, New York 1982
34. H. Steininger, S. Lehwald, H. Ibach, Surf. Sci. 123, 264 (1982)
35. J.S. Luo, R.G. Tobin, D.K. Lambert, G.B. Fisher, C.L. DiMaggio, Surf. Sci. 274, 53 (1992)